

In situ investigation with neutrons on the evolution of γ' precipitates at high temperatures in a single crystal Ni-base superalloy

R. Gilles¹, D. Mukherji², H. Eckerlebe³, P. Strunz⁴, J. Rösler²

¹ Technische Universität München, Forschungsneutronenquelle

Heinz Maier-Leibnitz (FRM II), Lichtenbergstr. 1, 85747 Garching, Germany

² Technische Universität Braunschweig, IfW, Langer Kamp 8, 38106 Braunschweig, Germany

³ GKSS Forschungszentrum Geesthacht, Max-Planck-Str. 1, 21502 Geesthacht, Germany⁴ Nuclear Physics Institute and Research Center Řež, 25068 Řež near Prague, Czech Republic

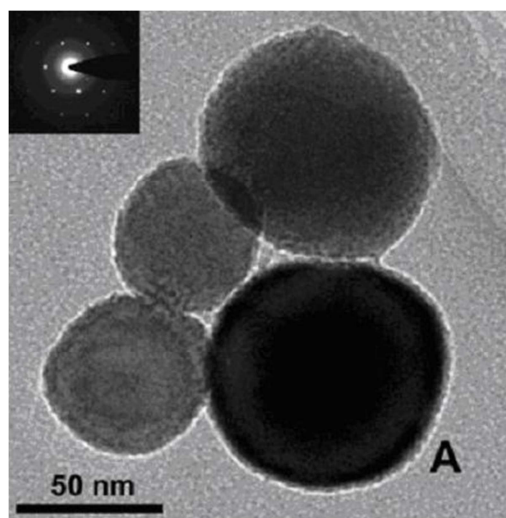
Key words: Neutron scattering, SANS, superalloys

Abstract. Single crystal Ni-base superalloys based on the γ / γ' system are widely used in gas turbine applications. To understand the formation of γ' precipitates, including size distribution and growth, we performed in situ small-angle neutron scattering (SANS) measurements at elevated temperatures and - together with TEM as well as SEM imaging - studied changes in the precipitates in short and long time scale. In the early stages, a bimodal size distribution of precipitate is observed, which (depending on the annealing temperature) changes to a cuboidal or nearly spherical morphology with almost unimodal size distribution.

Introduction

For gas turbine applications, materials with high temperature strength, e.g. single crystal Ni-base superalloys based on the γ / γ' system are used. Typically, the microstructure contains a high volume fraction (50 to 70%) of the cuboidal precipitates of Ni_3Al (γ' – ordered L1_2 structure) phase in a Ni solid solution matrix (γ – fcc structure). The precipitates are relatively large (500 nm) and they are regularly arranged along the $\{100\}$ directions in a 3D array, with narrow γ channels in between. The γ' precipitates form at high temperatures and they nucleate rather fast. Even a very rapid quenching from the single γ phase (solutioning temperature) can not suppress the nucleation of the Ni_3Al precipitates during cooling. A unimodal and perfectly aligned precipitate structure is desirable for improved mechanical properties of the superalloys, particularly the high-temperature creep, as such a structure is expected to be thermodynamically more stable.

In Fig. 1, some Ni_3Al -type nano-particle (~ 50 nm) extracted from a typical Ni-superalloy, clearly



show distribution in particle sizes. In the electrolytic selective phase dissolution process [1] that was adopted for the extraction of the nano-particles, the size was actually controlled in the base alloy prior to the extraction. Suitable heat treatment was adopted to control the size of the Ni_3Al -type precipitates in the Ni-base superalloy. These precipitates are coherent with the matrix [2] and their size, shape and distribution is a result of a complex interaction of the lattice misfit between the matrix and the precipitate and the process of precipitate growth (Ostwald ripening) at high temperatures [3,4]. Further, the cooling down step from the high temperature is also critical. For the extremely fine sizes mostly desired in the nano-particle synthesis (< 20 nm), the nucleation step of precipitates at the high temperature is a critical condition for the size

Fig. 1: TEM image of extracted Ni_3Al nano-particles.

control of the nano-particle. Conventional microscopic techniques do not allow effective study of the precipitate behaviour at very high temperatures and in the bulk of the sample. In-situ measurements with small-angle neutron scattering (SANS) as a probe makes a complete observation of the nucleation and growth of precipitates at high temperatures possible. Various publications show how size distribution, volume fraction, morphology, dissolution or rafting changes under the influence of temperature can be measured [5-9]. In this study, in-situ SANS measurements were performed to gain knowledge on the nucleation and the growth in the early stages of γ' precipitation, in an experimental single crystal alloy (tungsten rich Ni-base superalloy designated W3SX [10]). The results provide a possibility to estimate size of the precipitate nucleus. In-situ measurement at the high temperature is valuable as cooling from the high temperature can produce undesirable secondary precipitation, which in-adversely broaden the particle size distribution. Therefore, in our study one of the goals was to study the cooling effect on the precipitate size distribution. Once the volume fraction of the precipitate phase is effectively saturated at high temperature and a relatively slow cooling procedure is adopted, a unimodal distribution of particles can be produced.

Experimental

Sample designated W3SXST (W3SX alloy with nominal composition of Ni – 11.6 Al – 2.4 Ta – 3.5 W – 6.0 Cr – 1.3 Mo in at. % after solution heat treatment at 1260°C for 3h and water quenched) was used for the in-situ measurements. In Ni-base superalloys, the lattice misfit between the matrix and the precipitates influence the particle shape, size and size distribution and controls the final precipitate morphology. The in-situ measurement was used to follow the evolution of the Ni_3Al precipitates in W3SXST samples, in order to study the influence of temperature and internal strain on the precipitate morphology.

The measurements were performed with the SANS-2 instrument [11] at the Geesthacht Neutron Facility (GeNF). Selector-monochromated neutrons with a mean wavelength of $\lambda = 0.58$ nm and a wavelength spread of $\Delta\lambda/\lambda = 10\%$ were used. The neutron beam impinging on the samples had a diameter of 8 mm. The samples were heated in the neutron beam up to 1000°C with the heating rate of 5 K min⁻¹ using a special in-situ furnace. Samples of coin shape (12 mm radius and 2 mm thickness) were installed in the furnace. The beam passed thin Al and Nb windows in front and behind the sample.

The solutionized (prior ex-situ heat treated) sample contained small precipitates. Three samples were selected for the in-situ SANS measurements and hold at three different temperatures 800°C, 900°C and 1000°C. The sample at 800°C was aged for 35 hours, the one at 900°C for 11.5 hours and the sample at 1000°C for 4 hours. The 1000°C sample was further hold at 970°C for 12 hours. Four different detector distances (1 m, 3 m, 9 m, and 22 m) were used together with appropriate collimations to cover scattering vector magnitudes q from 0.02 to 2.5 nm⁻¹ ($q = 4\pi\sin(\theta)/\lambda$, where 2θ is the scattering angle). Scattered neutrons were recorded with a 50×50 cm² area detector with 256×256 pixel resolution. Measured intensities were corrected for sample transmission, background intensity, and detector response. The scattering cross section was calculated according to

$$\frac{d\Sigma}{d\Omega}(q, \alpha) = \frac{I(q, \alpha)}{I_0 D \Delta\Omega(q, \alpha) T} \quad (1)$$

$I(q, \alpha)$ is the measured intensity within a detector pixel, i.e. a solid angle element $\Delta\Omega$, I_0 is the intensity of the primary beam, D is the sample thickness, and T is the sample transmission, α is the angle between the scattering vector q and the reference direction of the sample (e.g. the crystal growth direction). The scattering vector q describes the directional change of a neutron in the scattering event. The absolute value of q is given by the scattering angle θ (angle between the incoming and the scattered neutron) and the wavelength λ as mentioned above. Absolute cross sections were calculated by comparison with incoherent scattering of vanadium.

The SANS scattering cross sections are analysed by means of a so-called two-phase model according to Kostorz [12],

$$\frac{d\Sigma}{d\Omega}(q) = (\Delta\eta)^2 \int_0^{\infty} n(R) V(R)^2 F(q, R)^2 dR, \quad (2)$$

where $d\Sigma/d\Omega$ represents the macroscopic differential scattering cross section. $\Delta\eta$ is the difference in the scattering length densities of particle and matrix, $n(R)dR$ stands for the number density of particles with sizes between R and $R+dR$, $V(R)$ is the volume of the particles, and $F(q, R)$ is the form factor of the particles. The particle form factor with $F_s(q, r)$ for spherical particles is [13]:

$$F_s(q, r) = 3 \frac{\sin(qr) - qr \cos(qr)}{(qr)^3}, \quad (3)$$

Often, the particle size distribution $n(R)$ can be described by an analytic function. An adequate choice can be a lognormal distribution, given by:

$$n(R) = \frac{n_0}{\sqrt{2\pi}\beta R_0} \cdot \exp\left(-\frac{(\ln(R/R_0))^2}{2\beta^2}\right) \quad (4)$$

The three free parameters of this distribution are the position of the maximum, R_0 , the width of the distribution, β , and the total number density of particles contained in the distribution, n_0 . The volume fraction of particles contained in the distribution is:

$$f = \int_0^{\infty} n(R) V(R) dR. \quad (5)$$

The two-dimensional data were azimuthal averaged and fitted under the assumption of a spherical approximation model. The parameters of the distributions are determined by fitting the scattering curve calculated by equation 3 to a measured scattering curve by means of a least-squares procedure.

Results and discussion

In Fig. 2 are SEM images of the W3SX alloy at the initial state before the in-situ heating (i.e. W3SXST condition) and the three images at room temperature (RT) after in-situ SANS, i.e. ageing at 800°C, 900°C and 1000°C, respectively. Before in-situ heating was performed the alloy has a bimodal size distribution with around 10 nm spherical and around 100 nm cuboidal precipitates (Fig. 2a). In the sample which was heat treated at 800°C for 35 hours and cooled down to RT again, the size distribution of the precipitates changed to a almost unimodal size distribution of nearly spherical precipitates with size of about 100 nm (Fig. 2b). Ageing at 900°C for 11.5 hours (after cooling to RT) results also in a nearly unimodal size distribution, with spherical particles of around 120 nm size (Fig. 2c). A few precipitates agglomerates to larger sizes greater than 200 nm. The sample aged at 1000°C and cooled to RT yields a bimodal size distribution with large cuboidal precipitates of more than 200 nm and a very fine spherical precipitates (Fig. 2d).

The change in the scattering curves with holding time was monitored at 1000°C to observe the evolution of the precipitate morphology. For this, the first scattering pattern during SANS measurement was taken immediately after reaching the temperature of 1000°C. Thereafter each 45 minutes a new pattern was recorded. This time frame was necessary to obtain a sufficient statistic for the weakly scattering W3SX alloy and to cover three/four different sample to detector distances. In Fig. 3 the differential cross section versus magnitude of the scattering vector q is plotted for various times (0.75, 1.5, 7.5, 12 and 15.75 hours) at 1000°C. Similar measurements were also done during holding at 800°C and 900°C. In order to follow the growing of precipitates, differences were taken between the first and the subsequent measured scattering curves at the fixed hold temperature.

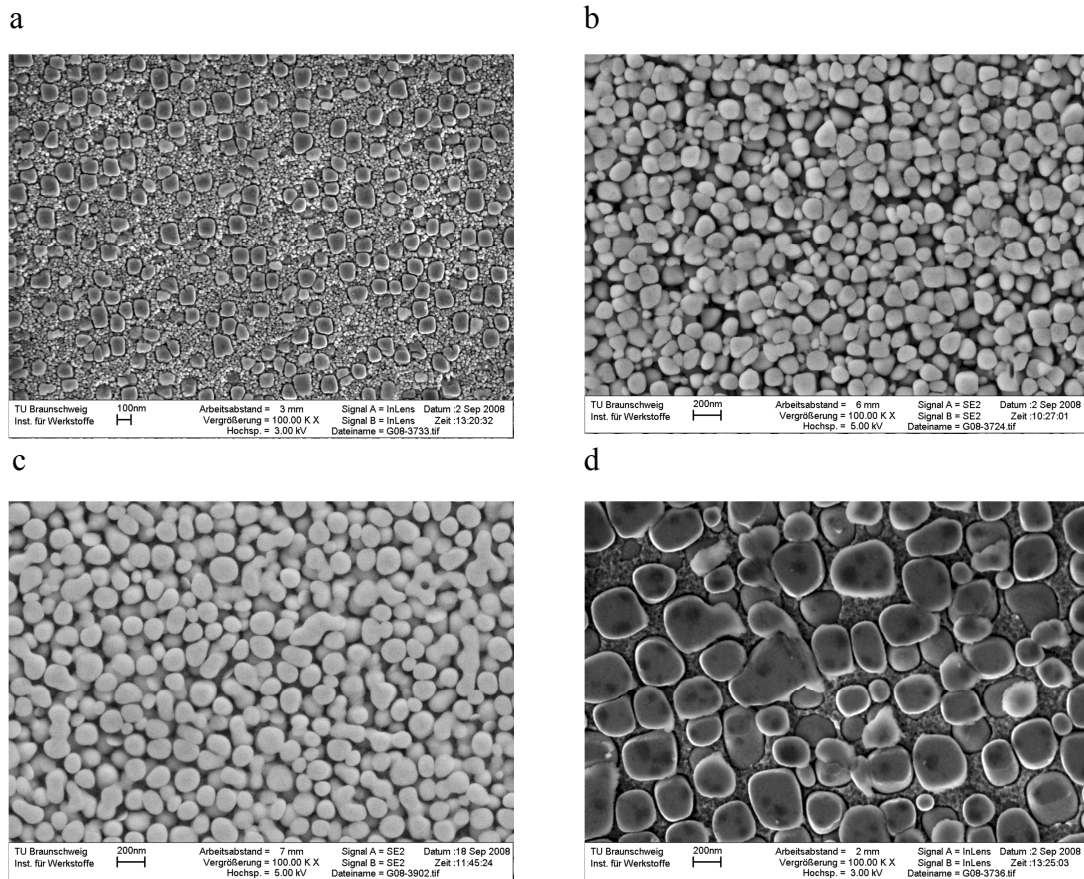


Fig. 2: SEM images of a) initial state before in-situ heating: bimodal size distribution: ~ 10 nm spherical and ~ 100 nm cuboidal precipitates, b) after heating to 800°C for 35 hours: unimodal size distribution: ~ 100 nm nearly spherical precipitates, c) after heating to 900°C for 11.5 hours: nearly unimodal size distribution: ~ 120 nm precipitates and agglomeration of a few precipitates to > 200 nm size and d) after heating to 1000°C for 4 hours + 970°C for 12 hours: bimodal size distribution: ~ 200 nm larger cuboidal and very fine spherical precipitates.

A different growth characteristics of the larger and the smaller precipitates could be observed, which provided a clue – on how to obtain a fine and mono-dispersed Ni_3Al precipitates in the alloy. Depending on the hold temperature and time, different precipitate size distributions were achieved in the alloy. All holding experiments started with precipitates of around 150 nm and kept this value for 800°C ageing. A small increase at 900°C is recognized, while 1000°C showed a strong change in the mean size of precipitates, growth up to 350 nm. In addition, some small precipitates were also detected on ageing at 1000°C but not at 800°C and very fine precipitates (around 2 nm) at 900°C which are stable in size during the holding time (Fig. 4). The source of these fine fractions are not clear at the moment.

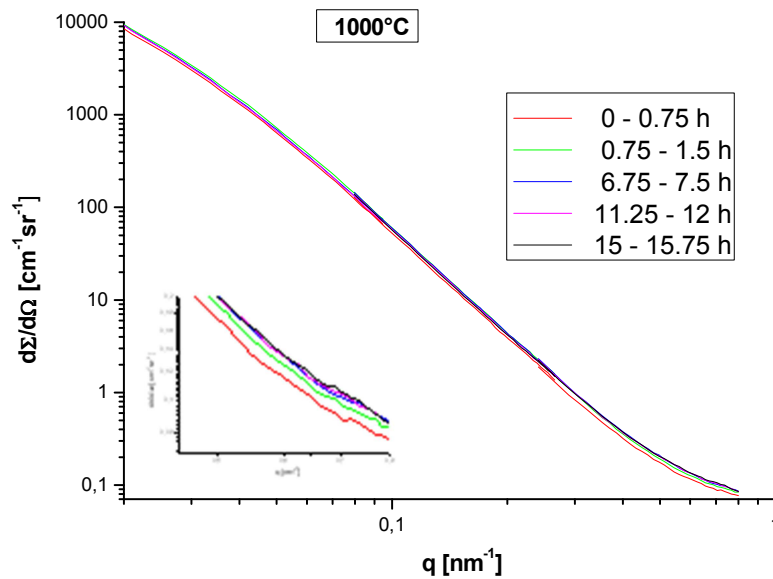


Fig. 3: Azimuthally averaged differential cross section versus q for changes after starting to hold the temperature at 1000°C. The inset is a magnification of higher q values to clarify the changes in the differential cross section (from the bottom up: start to hold up to increasing time of ageing hours) .

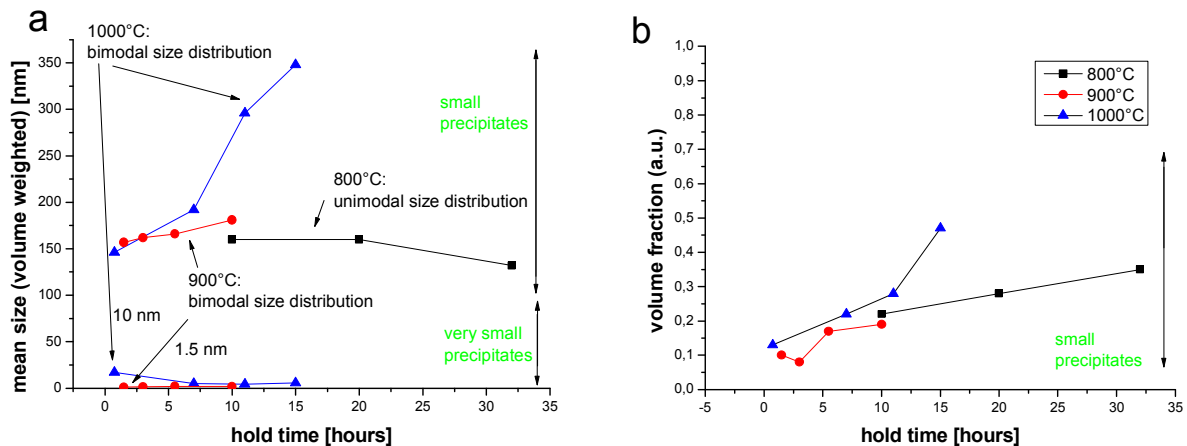


Fig.4: a) Mean size of small precipitates versus hold time (changes after starting to hold the temperature). b) Volume fraction of small precipitates versus hold time.

The starting bimodal size distribution in samples before the in-situ heating is caused by the cooling from the high temperature of 1260°C after the solution treatment, which results in very small new precipitates. The quenching is not fast enough to suppress the precipitation of secondary γ' . This is also observed during cooling from the highest in-situ heating temperature of 1000°C (Fig. 2a). It has to be mentioned that a direct comparison of size measured from SEM and SANS is not possible because the SANS values are volume weighted size distributions, which leads in general to small deviations.

Summary and Outlook

The combination of SANS and microscopic measurements allows us to follow the growth of precipitates at different temperatures. In the region of 800°C and 900°C the smaller precipitates grow to form a nearly unimodal size distribution which remains nearly spherical in shape. Nevertheless, a small size distribution of very fine secondary precipitates was observed by SANS at 900°C. At the elevated temperature of 1000°C, the volume fraction of the very small precipitates decreased and the precipitate morphology of larger precipitates changed to a cuboidal shape as seen after cooling to RT by SEM imaging. After cooling from 1000°C, new spherical precipitates are formed leading to a bimodal size distribution of the precipitate. The SEM images could only describe the initial and the final states of the sample at room temperature and can not monitor precipitate evolution at the high temperatures, especially the change in volume fraction. This was made possible by the in-situ SANS measurements which could also be used to monitor the changes during the cooling process. At all three holding temperatures the volume fraction for the precipitates above 100 nm increased by a factor of 2 to 3 during the ageing.

In a next step synchrotron measurements will be performed to observe to more closely monitor the formation of precipitates during cooling from the single phase region and then the growth at the high temperature is started. Faster detector and improvements in furnace heating and cooling rates will allow to measure in time frames of a few seconds instead of the 45 minutes that was required for the SANS measurement. After in-situ solutioning at 1260°C, it will be possible to follow by a rapid transfer to the ageing temperatures how the precipitates nucleate.

Acknowledgement

The authors like to thank M. Sharp (GKSS) and G. Kozik (GKSS) for support on the experiment and the furnace control. R. Gilles thanks GKSS for providing beam time and financial support.

References

- [1] D. Mukherji, G. Pigozzi, F. Schmitz, O. N  th, J. R  sler and G. Kostorz: *Nanotechnology* 16 (2005), p. 2176-2187.
- [2] R. Gilles, D. Mukherji, M. Hoelzel, P. Strunz , D.M. Toebbens, B. Barbier: *Acta Mat.* 54 (2006) p.1307-1316.
- [3] A. Baldan: *Journal of Materials Science* 37 (2002), p. 2379-2405.
- [4] C.S. Jayanth, P. Nash: *Journal of Materials Science* 24 (1989), p. 3401-3052.
- [5] P.Strunz, D.Mukherji, R.Gilles, A.Wiedenmann, J.R  sler, H.Fuess: *J.Appl.Cryst.* 33 (2001) p.541-548.
- [6] P. Strunz, R. Gilles, D. Mukherji, A. Wiedenmann: *J. Appl. Cryst.* 36 (2003) p. 854-859.
- [7] R. Gilles: *International Journal of Materials Research* 96 (2005), p. 325- 334.
- [8] D. Mukherji, R. Gilles, P. Strunz, S. Lieske, A Wiedenmann and R.P. Wahi: *Scripta Materialia*, Vol. 41, No. 1 (1999), p. 31-38.
- [9] D. Mukherji, P. Strunz, D. del Genovese, R. Gilles, J. R  sler, A. Wiedenmann: *Metallurgical and Materials Transactions A*, Vol. 34A (2003), p. 2781- 2792.
- [10] D. Mukherji and J. R  sler: *International Journal of Materials Research* 94 (2004), p. 478-484.
- [11] http://www.gkss.de/central_departments/genf/instruments/003124/index_0003124.html.de
- [12] G. Kostorz, in: *Neutron Scattering (Treatise on materials science and technology)*, ed. G. Kostorz, Academic Press, New York (1979), p. 227-289.
- [13] A. Guinier, G. Fournet: *Small-angle Scattering of X-rays*, John Wiley&Sons, Inc. (1955).